Raman, Brillouin, and nuclear magnetic resonance spectroscopic studies on shocked borosilicate glass

Murli H. Manghnani,[1] Anwar Hushur,[1] Toshimori Sekine,[2] Jingshi Wu,[3] Jonathan F. Stebbins,[3] and Quentin Williams[4]
[1]*University of Hawaii, Hawaii Institute of Geophysics & Planetology, Honolulu, Hawaii 96822, USA*
[2]*Hiroshima University, Department of Earth and Planetary Systems Science, Higashi-Hiroshima 739-5826, Japan*
[3]*Stanford University Department of Geological and Environmental Sciences, Stanford University, Stanford, California 94305, USA*
[4]*University of California at Santa Cruz, Department of Earth Sciences, Santa Cruz, California 95064, USA*

(Received 8 March 2011; accepted 15 April 2011; published online 2 June 2011)

Using Brillouin and Raman scattering and NMR techniques, we have investigated the elastic and structural properties of four post-shocked specimens of borosilicate glass, recovered from peak pressures of 19.8, 31.3, 40.3, and 49.1 GPa. The Raman spectra of shock-wave compressed borosilicate glass for peak pressures of 19.8 and 31.3 GPa show two new peaks at 606 cm^{-1} and near 1600 cm^{-1}, while a peak at ~923 cm^{-1} disappears in these glasses following shock-loading. The mode at 606 cm^{-1} is correlated with four-membered rings, composed of one BO_4 and three SiO_4 tetrahedra (a reedmergneritelike configuration). Modes near ~1600 cm^{-1} are of uncertain origin, while that at 923 cm^{-1} may associated with silica tetrahedra with two nonbridging oxygens, although standard models of this type of glass suggest that total nonbridging oxygen contents should be low. The Raman spectra for the shocked samples at 40.3 and 49.1 GPa are similar to that of the unshocked sample, suggesting that much of the irreversible density and structural changes are recoverable following adiabatic decompression and thermal relaxation. This reversibility for the highest pressure shocked samples is in accord with the Brillouin results, which show an increase in the product of sound velocity and index of refraction at pressures up to 20 GPa. The Raman band initially at 450 cm^{-1}, which corresponds to the bending vibration mode of the Si–O–Si, Si–O–B (with primarily six-membered rings in the network) reaches a maximum frequency of 470 cm^{-1} and narrowing at a peak shock pressure of 31.3 GPa, and then also decreases to its initial values for samples shocked at 40.3 and 49.1 GPa. This shift toward higher frequency under shock-wave compression indicates the average Si–O–Si, Si-O-B angles decrease with pressure. The narrowing of this band suggests a narrower distribution of Si–O–Si angles in the shocked samples for peak pressures of 19.8 and 31.3 GPa. ^{11}B NMR spectra for all four shocked glasses are similar, and indicate ratios of BO_3 to BO_4 that are not greatly changed from the starting material. However, changes in peak shapes suggest significant changes in the connectivity of the B and Si components of the network, with more silicon neighbors surrounding BO_4 tetrahedra in the shocked glasses, and a modest increase in the number of nonring related BO_3 groups following shock-loading. Thus, the irreversible effects of shock-loading appear to be to generate smaller rings of tetrahedra (hence decreasing the average T–O–T bond angle), and to increase the average number of neighbors of Si around boron tetrahedra. © *2011 American Institute of Physics*. [doi:10.1063/1.3592346]

I. INTRODUCTION

Borosilicate glasses are used as transparent armors, precision engineering materials, neutron absorbers, optical mirrors and display glasses because of their many unusual properties such as high failure strength and excellent optical transparency. They are also the leading and most intensively studied candidate medium for immobilizing nuclear waste. An enhanced understanding of the glass structure and its responses to pressure and temperature can maximize the effective use of glasses for different applications. For example, a fundamental understanding of glass structure, elastic properties and strength under *in situ* static and dynamic high pressures is the key for deployment as armor ceramics.

In high-pressure studies of borosilicate glasses, several shock-wave experiments have been carried out to probe the nature and effects of the shock process.[1–5] These studies show several different regions in the stress-time profile of borosilicate glasses. At pressures below 3 GPa, a nonlinear elastic response is found, while an approximately linear elastic response is present at pressures between 3 and 7.5 GPa. For shock pressures above 7.5 GPa, the glass shows viscoplastic behavior. Several impact and penetration studies on borosilicate glasses[6] show delayed failure in the glass due to the propagation of a failure wave. Studies on the structural changes in borosilicate glass induced by shock-wave compression are important for understanding the detailed shock-wave process in the glass, and the structural behavior of the

 © 2011 American Institute of Physics

Downloaded 17 Jan 2012 to 133.41.74.97. Redistribution subject to AIP license or copyright; see http://jap.aip.org/about/rights_and_permissions

glass under dynamic compression. However, no structural studies have been carried out on shock-recovered borosilicate glasses and at present there is insufficient knowledge to understand the structural changes that occur in these glasses during shock-wave compression.

Raman scattering provides direct information on the pressure induced changes in the glass structure (i.e., bond length, bonding angle, and densification) which can be correlated with glass strength. Raman spectroscopy has been applied to probe the structure and dynamics of glasses in numerous studies.[7] The Raman spectra of pressure-densified fused silica have been reported by several workers.[8–11] The densification processes in SiO_2, obsidian, anorthite glasses and quartz induced by shock-wave compression have been studied by Raman spectroscopy.[12–15]

In the present study, we have investigated four shock recovered borosilicate samples, shocked to peak pressures of 19.8, 31.3, 40.3, and 49.1 GPa, using Raman, Brillouin and NMR spectroscopy. These data yield information on the structural changes and densification (or lack thereof) in the shocked samples.

II. EXPERIMENTAL

Four shock-recovered samples of borosilicate glasses (disks of about 0.9 mm thickiness and 10 mm diameter) are used for this study. The samples were shocked using a single stage propellant gun; samples were enclosed in a steel container (stainless steel 304), and peak pressures were calculated from projectile velocities using impedance matching.[16] 3-mm thick stainless steel 304 was employed as flyer material at impact velocities of 0.95, 1.41, 1.74, and 2.04 km/s, corresponding to peak shock pressures of 19.8, 31.3, 40.3, and 49.1 GPa, respectively. The sample cavity was located 3-mm deep from the impact surface of the container (30 mm long, 30 mm diameter). Shocked glasses were recovered as intact (albeit fractured) glass disks. The glass composition is given in Table I; the atomic Si/B ratio in the glass is ~3.7, and the overall composition is that of commercial Pyrex®. Clear fragments of glass, free of visible bubble and inclusions, were obtained from all but the highest pressure runs. Their densities were measured by the sink-float method in acetone-diiodomethane mixtures[17] and were found to be the same within an uncertainty of about ± 0.7%, suggesting significant relaxation from their high-pressure/temperature state.

Raman spectra were obtained with a confocal DILOR XY micro-Raman spectroscopy using the 514.5 nm green line of a Spectra Physics Ar-ion laser for sample excitation. The incident laser light is focused using a 50 × long distance objective which gave a spot size of ~2–3 μm at the sample. Laser power at the sample was 30 mW, and the scattered light was collected using the same objective and detected by a CCD detector.

TABLE I. Composition of borosilicate glass used in this study. It also includes minor amounts (less than 1 wt. %) of MgO, SO_3, TiO_2, SrO, MnO, and Cr_2O_3.

SiO_2	Al_2O_3	Fe_2O_3	CaO	Na_2O	K_2O	ZrO_2	BaO	B_2O_3
80.54	2.53	0.015	0.02	3.54	0.64	0.03	0.02	12.70

TABLE II. Elastic properties of borosilicate glass at ambient temperature and pressure obtained in this study.

Glass sample	Density (g/cm^3)	V_p (km/s)	V_s (km/s)	G(GPa)	K_s(GPa)	E(GPa)	Poisson's ratio
Borosilicate	2.242	5.561	3.422	26.248	34.324	62.749	0.195

The Brillouin scattering experiments were also conducted using a similar laser. The output beam power is 130 mW, and at the sample, beam power is 60 mW. Brillouin spectra were taken in backscattering geometry using a lens with 6 cm of focal length. No polarizer was used for detecting the scattered light.

^{11}B MAS NMR spectra for all of the glasses were collected on a Varian 14.1 T spectrometer at 192.4 MHz using a Varian/Chemagnetics T3 probe with 3.2 mm zirconia rotors spinning at 20 kHz with a recycle delay of 1 s and a radio frequency pulse length of 0.3 μs, which corresponds to a liquid radio frequency (rf) tip angle of about $\pi/16$. ^{11}B chemical shifts are reported in parts per million (ppm) relative to 1.0 M boric acid at 19.6 ppm. For the ambient pressure and 19.8 GPa samples, ^{27}Al MAS spectra (not shown here) were collected with the same instrument with similar conditions and also with a similar probe at 18.8 T. Triple-quantum MAS spectra were also collected at 14.1 T as recently described.[18] In both cases, only a single peak for four-coordinated Al (^{IV}Al) was observed; no peaks for ^{V}Al or ^{VI}Al, which is common in densified, high pressure aluminosilicate glasses,[18] were seen at a detection limit of about 1%, consistent with results of Prasad *et al.*[19] on ambient pressure Pyrex® glass.

III. RESULTS AND DISCUSSION

A. Raman and Brillouin spectra of unshocked and shocked samples

Figure 1 shows typical Raman spectra of the unshocked borosilicate glass at ambient temperature and pressure. As expected from the high silica content of the glass, the main features of the spectrum are very similar to the spectrum of

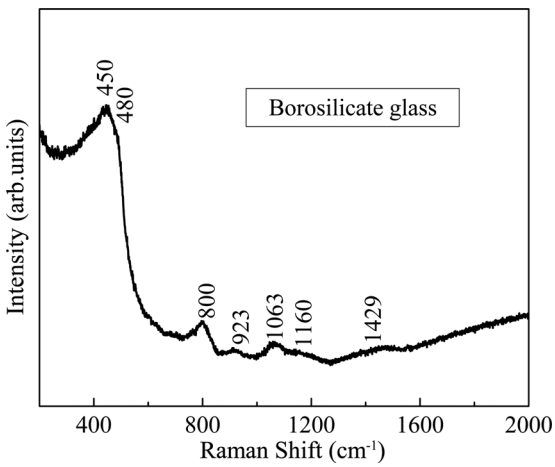

FIG. 1. Raman spectra of borosilicate glass at ambient condition.

Downloaded 17 Jan 2012 to 133.41.74.97. Redistribution subject to AIP license or copyright; see http://jap.aip.org/about/rights_and_permissions

pure silica glass.[20,21] The intense broad band at around 450 cm^{-1} dominates the Raman spectrum. A shoulder is also visible at 480 cm^{-1}. Other modes are observed at 800, 923, 1063, and 1160 cm^{-1}. The band assignments of the Raman spectra can be based on previous work on SiO_2 glass and SiO_2-rich glasses (i.e., Pyrex®, borosilicate and various alkali silicates).[7,20–26] The 450 cm^{-1} Raman band is assigned to the bending vibration mode of the Si–O–Si bond (T–O–T bending mode of the TO_4 network structure) in six-membered rings. The 480 cm^{-1} band has been assigned to a vibrationally isolated Si–O–Si, Si–O–B mode of four-membered rings which has small inter-tetrahedral angles. The weak band at around 800 cm^{-1} is assigned to the O–Si–O symmetric bond stretching, associated with motions of Si (possibly also B) against its O cage. Narrow bands near to 806 cm^{-1} have also commonly been assigned to three-membered rings of BO_3 triangles ("boroxyl rings") in borate and other glasses,[23,26] but the shape of this feature in the Pyrex®-based glasses and their composition suggests that this species may not be abundant. The 923 cm^{-1} band is attributed to a Si–O stretching vibration with two nonbridging O atoms per silicon. The bands at 1063 and 1160 cm^{-1} are respectively assigned to the Si–O stretching in a tetrahedron with one nonbridging oxygen per silicon, and a fully polymerized tetrahedron. It is important to note, however, that conventional models of alkali borosilicate glass structure[27] suggest that there should be no nonbridging oxygens (NBO) in this composition range. Our ^{11}B measurements (below) support this approximation, suggesting that the total concentration of nonbridging oxygens (NBO) is probably less than 1 or 2% of total oxygens, and that the concentrations of the corresponding Si and B species should thus also be quite low, although possibly detectable by Raman spectroscopy.

The Raman spectrum of the four shocked samples and the ambient pressure sample is presented in Fig. 2. The Raman spectra of shock compressed borosilicate glass for peak pressure 19.8 and 31.3 GPa shows new peaks at 606 $cm^{-1}$and near 1600 cm^{-1}. In pure silica glass, there is a mode at 606 cm^{-1} which has been assigned to a "defect"

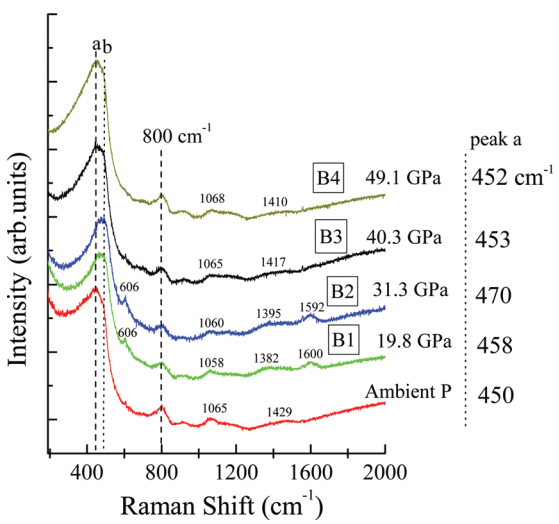

FIG. 2. (Color online) Raman spectra of shock recovered samples of borosilicate glass.

band involving either partially broken bonds or three-membered rings of SiO_4 tetrahedra.[21] In borosilicate glasses with a relatively low ratio of Si/B, a mode at 630 cm^{-1} have been observed and attributed to the breathing mode of danburite-like rings (four-membered rings that contain two SiO_4 and two BO_4 tetrahedra).[23,28] These authors also discussed the possible connection of this 630 cm^{-1} mode to the breathing mode of reedmergneritelike rings, which include three SiO_4 and one BO_4 tetrahedra. The mode associated with four-membered rings in danburite ($CaB_2Si_2O_8$) is observed at 614 cm^{-1}, while the mode related to the four-membered rings in reedmergnerite ($NaBSi_3O_8$) is observed at 586 cm^{-1}. The 606 cm^{-1} mode in our shocked borosilicate glass sample thus lies between the modes for reedmergnerite rings and danburite rings. Considering the high Si/B ratio of our borosilicate sample and the NMR results discussed below, we conclude that the mode which appears at 606 cm^{-1} in glasses shocked to a peak pressure of 19.8 and 31.3 GPa is associated with reedmergneritelike, four-membered tetrahedral rings. The presence of such smaller rings is generally viewed as correlated with increased density of silica-rich glasses, e.g., Refs. 11, 29, 30.

The new modes at ~1600 cm^{-1} are higher in frequency than generally reported in borosilicate glasses. Raman bands at about 1500 to 1550 cm^{-1} have been attributed to B–O stretching vibrations involving NBO in Na-rich borate glasses,[23,24,31] but again, the NBO concentration in the Pyrex® composition should be very low. Bands in this region have also been associated with boroxyl ring modes.[24] It has been suggested that decreases in the Si–O–Si angles between corner-shared silicate tetrahedra in glasses and melts with increasing pressure can lead to arrangements of oxygen atoms to the edge- or face-shared octahedra.[32] Indeed, Raman bands at about 1350 and 1600 cm^{-1} in the spectra for fully vitrified retrieved silica have been attributed to Si–O bond stretching in the bipyramidal cage of six O atoms.[33] The mode at ~1600 cm^{-1} in our study may be related to the Si–O bond stretching in the higher coordinated polyhedra. The Raman spectra for the shocked samples at 40.3, 49.1 GPa are similar to the unshocked sample in this region, implying that watever their exact nature, these B–O or Si–O species are destabilized by post-shock high temperatures. The Raman band at 450 cm^{-1} corresponds to the bending vibration mode of the Si–O–Si and Si–O–B six-membered rings in the network. This band reaches a maximum (470 cm^{-1}) at a peak shock pressure of 31.3 GPa, and then decreases in frequency for the samples shocked at 40.3 and 49.1 GPa (Fig. 3). In addition, the 450–480 cm^{-1} band for peak pressures of 19.8 and 31.3 GPa became narrower as compared to the unshocked and shocked samples (40.3, 49.1 GPa): a result that mirrors the behavior of silica glass under static compression.[34] Interestingly, static high-P Raman measurements in the diamond anvil cell show that the 450 cm^{-1} band (at ambient P) is shifted to ~470 cm^{-1} at ~1.3 GPa.[35] Since the 450 cm^{-1} band is related to the average T–O–T bond angle (the Si–O–Si and Si–O–B angles, primarily in six-membered rings of tetrahedra), a shift toward higher frequency following shock-compression indicates that the average bond angle decreases with pressure, implying

Downloaded 17 Jan 2012 to 133.41.74.97. Redistribution subject to AIP license or copyright; see http://jap.aip.org/about/rights_and_permissions

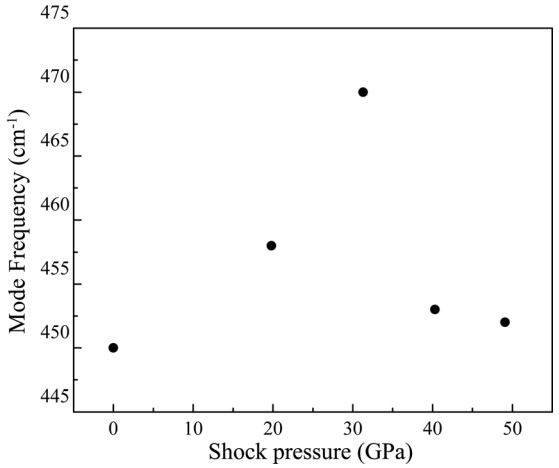

FIG. 3. Raman frequency of 450 cm^{-1} Band vs peak shock pressure.

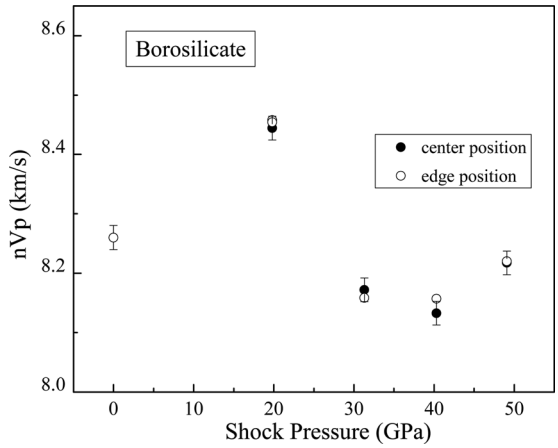

FIG. 4. nV_p of shock densified borosilicate glasses. n is refractive index of the shocked glass.

that an irreversible structural modification in the glass has taken place. The narrowing of the 450–480 cm^{-1} band suggests a narrower distribution of Si–O–Si angles in the shocked samples for peak pressures of 19.8 and 31.3 GPa. Taken in tandem with the observation of a new band near 606 cm^{-1}, the irreversible effect of shock compression appears to be to both generate smaller rings and to narrow the T–O–T bond angle.

As noted in the experimental section, the measured densities of the shocked and unshocked glasses are the same within 0.7% uncertainty. This suggests significant post-shock relaxation, as density increases of borosilicate and aluminosilicate glasses melted and compressed statically even to pressures less than 10 GPa often exceed 5 to 10%.[17]

For static high-pressure measurements, the frequency changes of the 450 cm^{-1} band are generally correlated to the densification at high pressure. However, the frequency variations of the 450 cm^{-1} Si–O–Si bending mode in these shock-quenched glasses are not correlated with measurable density changes of the shock-recovered samples. While the environment of the Si atoms appears to have undergone alterations typically associated with densification, the differences in static and shock-wave compression may result from structural modifications associated with boron in these shocked samples. In this context, the appearance of a new Raman band at 1600 cm^{-1} may indicate that shifts in the environment of boron may provide a competing and compensating effect with respect to density shifts for the angle changes and shifts in ring size undergone by portions of the silica network. Thus, to probe both the elastic behavior of these glasses and the local environment of boron, both Brillouin spectra and NMR measurements were made on these samples.

In Fig. 4, the longitudinal sound velocity V_p times the refractive index n is shown as a function of pressure for these glasses, as determined from Brillouin spectroscopy. The open circles are the data points taken at the edge position of the sample, while the dark circles represent the data measured at a central position. The rationale for these two sets of measurement is simply to monitor whether the edges of the samples, which likely underwent more rapid cooling in the post-shock environment show any systematic or resolvable difference in properties from those at the center of the sample. The product of nV_p shows an increase to a maximum at peak pressure 19.8 GPa, followed by a decrease for higher peak pressures than 19.8 GPa: the highest pressure data actually lie below the ambient pressure value (Fig. 4). For comparison, the variations of refractive index and density of SiO_2 glass recovered from different shock pressures have been reported.[13] These show a maximum near ~26 GPa (with values at pressures below ~10 and above ~33 GPa estimated to be near the ambient pressure values), and have very similar behaviors with shock pressure. The maximum density increment observed by Okuno *et al.*[13] is 11.0% for a peak shock pressure of 26.3 GPa, while the maximum refractive index increment is 3.23%. For shocked borosilicate glasses, the close relationship between density and refractive index through the Lorentz–Lorenz relationship implies that the refractive index of the shocked glasses has also not changed significantly. Hence, the increase in velocity and longitudinal elastic constant for the borosilicate glass sample shocked to 19.5 GPa is most likely related to structural modifications of the silicate-dominated network (for example, the appearance of reedmergneritelike rings and the probable narrowing of the Si–O–Si angle within six-membered rings of tetrahedra). Thus, while the density of these glasses is not resolvably changed following shock-loading, the longitudinal elastic modulus is clearly elevated by ~5% in the 19.5 GPa glass.

B. NMR spectroscopy

There have been numerous NMR studies on borosilicate glasses,[36–41] including a few published on Pyrex® glass[19,36] which is the same type of composition as was used in this study. ^{11}B NMR spectra for all four shocked glass samples and unshocked sample are shown in Fig. 5. All ^{11}B NMR spectra are similar, and indicate that the contents of BO_3 and BO_4 groups are not greatly changed from those of the starting material. The fraction of the latter is about $22 \pm 1\%$ of the total boron species. From the reported composition, this figure is consistent within error of the standard borosilicate glass model assumption[27] that in this compositional range, the added Na_2O converts BO_3 groups to BO_4 without

Downloaded 17 Jan 2012 to 133.41.74.97. Redistribution subject to AIP license or copyright; see http://jap.aip.org/about/rights_and_permissions

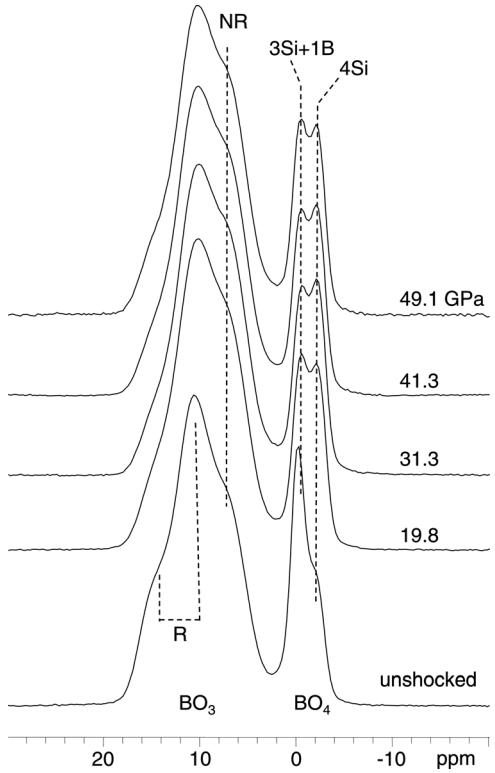

FIG. 5. ^{11}B MAS NMR spectra (14.1 T) of shocked and unshocked glasses. Peaks for BO_4 groups with four Si and with three Si and one B neighbors, and for BO_3 groups in three-membered rings ("R," quadrupolar doublet) and not in three-rings ("NR," shoulder) are labeled.

generating significant fractions of NBO. This conclusion is valid if "nonstandard" species, such as oxygen "triclusters" of three BO_4 groups, and high-coordinated Al (AlO_5 or AlO_6 groups) are negligible. There is no evidence for the former in these types of glasses; our high-field ^{27}Al NMR data (see experimental section) limit the latter to less than about 1%.

On the other hand, the differences in the shapes of both the BO_3 and BO_4 peaks between the unshocked and shocked material are dramatic and, from previous studies,[19,40,41] can be attributed to previously characterized types of structural changes. The BO_3 peak is dominated by two components, each with a complex peak shape caused by the relatively large quadrupolar coupling constants typical of such groups. These can be assigned to a major component of BO_3 in rings (three BO_3 and/or BO_4 groups), and a minor component of "nonring" BO_3.[40,41] In contrast, BO_4 groups are well-known to have very small quadrupolar couplings, leading to narrow, Gaussian peaks at their characteristic chemical shifts. The shoulders and splittings of the BO_4 peaks are therefore usually attributed to variations in the numbers of first-neighbor cations, which in borosilicates are ascribed to varying numbers of B and Si. In particular, the two overlapping BO_4 components with peak positions near to –0.2 and –2.0 ppm are similar to those attributed to 1B, 3Si neighbors and 0B, 4Si neighbors, respectively,[40,41] which is sensible given the high Si/B ratio of the Pyrex® composition. Thus, it appears that the shocked glasses have a significantly increased fraction of nonring BO_3 groups, and of BO_4 groups with a higher number of Si neighbors. If some BO_4 groups are part of the three-membered ring species, than in fact these trends should be correlated, as conversion of ring to nonring species will lead to more Si neighbors on average. A similar change in both types of species was observed in annealing experiments on somewhat comparable alkali borosilicates, and connected to the development of long-range heterogeneity (incipient phase separation) at lower temperatures.[42]

It is thus possible that some of the difference between shocked and unshocked glasses observed by NMR is the result of the former having a higher fictive temperature, resulting from being heated well above the glass transition region along some P/T path and then cooling more rapidly than the starting glass after decompression. Finally, to test the reversibility of the changes induced in the shocked glasses, samples of the unshocked glass and the 19.8 GPa glass were heated to 550 °C (well above T_g) for 10 min, then cooled at 0.1 °C/s. The ^{11}B spectra were identical for both, and were very similar to the spectrum for the unshocked glass in Fig. 5.

IV. CONCLUSIONS

The Raman and NMR spectroscopy yield complementary pictures of the structural changes induced in shock-recovered Pyrex® composition glasses. The largest structural changes present within these glasses are induced by pressures less than 40 GPa: high post-shock temperatures for samples shocked to higher pressures plausibly produce reversion of irreversibly densified features due to post-shock annealing. Specifically, in the 19–31 GPa range, six-membered rings of tetrahedra have narrower Si–O–Si(B) angles and more four-membered rings (with three silicons and one boron tetrahedra) are present. Additionally, the number of silicon first neighbors surrounding BO_4 tetrahedra is enhanced. However, the abundance of a small fraction of silica tetrahedra with two nonbridging oxygens is significantly reduced in the shock-loaded samples. Thus, it appears that shock-loading induces complex structural changes within these glasses: while the shifts in bond-angle and ring statistics closely mirror pressure-induced changes that occur in silica glass, there may also be a net shift in the distribution nonbridging oxygens (and hence local polymerization) in the shock-loaded samples. Some of the recovered structural changes may also be attributable to variations in thermal history on decompression and cooling of the shocked glasses.

ACKNOWLEDGMENTS

This work was partially supported by the National Science Foundation (Grant No. EAR 05-38884). We thank John Balogh for maintaining our Brillouin and Raman scattering facility at the University of Hawaii. The borosilicate glass ("borofloat") samples were provided by Dr. Parimal Patel and Dr. Douglas Templeton under the TARDEC Contract No. DAAE07-01-C-L055. We thank Dr. Oliver Tschauner at the UNLV High Pressure Center and Dr. Dennis Grady for their valuable comments to the manuscript. SOEST and Hawaii Institute of Geophysics and Planetology contribution No. 8162/1888.

[1] J. Cagnoux, Bull. Am. Phys. Soc. **26**, 657 (1981).
[2] J. Cagnoux, Aip Conf. Proc. **78**, 392 (1981).

Downloaded 17 Jan 2012 to 133.41.74.97. Redistribution subject to AIP license or copyright; see http://jap.aip.org/about/rights_and_permissions

[3]N. K. Bourne, J. C. F. Millett, and J. E. Field, Proc. R. Soc. London, Ser. A **455**, 1275 (1999).
[4]X. Nie, W. W. Chen, X. Sun, and D. W. Templeton, J. Am. Ceram. Soc. **90**, 2556 (2007).
[5]C. S. Alexander, L. C. Chhabildas, W. D. Reinhart, and D. W. Templeton, Int. J. Impact Eng. **35**, 1376 (2008).
[6]N. K. Bourne, J. C. F. Millett, and Z. Rosenberg, J. Appl. Phys. **80**, 4328 (1996).
[7]P. F. McMillan, G. H. Wolf, and B. T. Poe, Chem. Geol. **96**, 351 (1992).
[8]G. E. Walrafen and P. N. Krishnan, J. Chem. Phys. **74**, 5328 (1981).
[9]P. McMillan, B. Piriou, and R. Couty, J. Chem. Phys. **81**, 4234 (1984).
[10]G. E. Walrafen, Y. C. Chu, and M. S. Hokmabadi, J. Chem. Phys. **92**, 6987 (1990).
[11]B. T. Poe, C. Romano, and G. Henderson, J. Non-Cryst. Solids **341**, 162 (2004).
[12]P. F. McMillan, G. H. Wolf, and P. Lambert, Phys. Chem. Miner. **19**, 71 (1992).
[13]M. Okuno, B. Reynard, Y. Shimada, Y. Syono, and C. Willaime, Phys. Chem. Miner. **26**, 304 (1999).
[14]B. Reynard, M. Okuno, Y. Shimada, Y. Syono, and C. Willaime, Phys. Chem. Miner. **26**, 432 (1999).
[15]K. Shimoda, M. Okuno, Y. Syono, M. Kikuchi, K. Fukuoka, M. Koyano, and S. Katayama, Phys. Chem. Miner. **31**, 532 (2004).
[16]T. Sekine, Eur. J. Solid State Inorg. Chem. **34**, 823 (1997).
[17]J. R. Allwardt, J. F. Stebbins, B. C. Schmidt, D. J. Frost, A. C. Withers, and M. M. Hirschmann, Am. Miner. **90**, 1218 (2005).
[18]K. E. Kelsey, J. F. Stebbins, D. M. Singer, G. E. Brown Jr., J. L. Mosenfelder, and P. D. Asimow, Geochim. Cosmochim. Acta **73**, 3914 (2009).
[19]S. Prasad, T. M. Clark, T. H. Sefzik, H.-T. Kwak, Z. Gan, and P. J. Grandinetti, J. Non-Cryst. Solids **352**, 2834 (2006).
[20]C. F. Smith, in *Borate Glasses: Structure, Properties, Applications* (Plenum, New York, 1978), p. 307.
[21]S. K. Sharma, T. F. Cooney, Z. F. Wang, and S. vanderLaan, J. Raman Spectrosc. **28**, 697 (1997).
[22]P. McMillan and B. Piriou, Bull. Miner. **106**, 57 (1983).
[23]D. Manara, A. Grandjean, and D. R. Neuville, Am. Miner. **94**, 777 (2009).
[24]T. Yano, N. Kunimine, S. Shibata, and M. Yamane, J. Non-Cryst. Solids **321**, 137 (2003).
[25]P. McMillan, Am. Miner. **69**, 622 (1984).
[26]W. L. Konijnendijk and J. M. Stevels, J. Non-Cryst. Solids **21**, 447 (1976).
[27]W. J. Dell, P. J. Bray, and S. Z. Xiao, J. Non-Cryst. Solids **58**, 1 (1983).
[28]B. C. Bunker, D. R. Tallant, R. J. Kirkpatrick, and G. L. Turner, Phys. Chem. Glasses **31**, 30 (1990).
[29]R. J. Hemley, H. K. Mao, P. M. Bell, and B. O. Mysen, Phys. Rev. Lett. **57**, 747 (1986).
[30]Q. Williams, R. J. Hemley, M. B. Kruger, and R. Jeanloz, J. Geophys. Res. **98**, 22157 (1993).
[31]H. Li, Y. Su, L. Li, and D. M. Strachan, J. Non-Cryst. Solids **292**, 167 (2001).
[32]E. M. Stolper and T. J. Ahrens, Geophys. Res. Lett. **14**, 1231 (1987).
[33]S.-N. Luo, O. Tschauner, P. D. Asimow, and T. J. Ahrens, Am. Miner. **89**, 455 (2004).
[34]T. Deschamps, C. Martinet, D. de Ligny, and B. Champagnon, J. Non-Cryst. Solids **355**, 1095 (2009).
[35]M. H. Manghnani, A. Hushur, and Q. Williams (unpublished).
[36]G. L. Turner, K. A. Smith, R. J. Kirkpatrick, and E. Oldfield, J. Magn. Res. **67**, 544 (1986).
[37]J. Zhong and P. J. Bray, J. Non-Cryst. Solids **84**, 17 (1986).
[38]P. J. Bray, Inorg. Chim. Acta **289**, 158 (1999).
[39]S. K. Lee, C. B. Musgrave, P. D. Zhao, and J. F. Stebbins, J. Phys. Chem. B **105**, 12583 (2001).
[40]L. S. Du and J. F. Stebbins, Chem. Mater. **15**, 3913 (2003).
[41]L. S. Du and J. F. Stebbins, J. Phys. Chem. B **107**, 10063 (2003).
[42]L. S. Du and J. F. Stebbins, J. Non-Cryst. Solids **315**, 239 (2003).

Downloaded 17 Jan 2012 to 133.41.74.97. Redistribution subject to AIP license or copyright; see http://jap.aip.org/about/rights_and_permissions